A Turbulent Burning Law Derived From Combustion Experiments

D.P. Hoult & V. H. Nguyen
Department of Mechanical Engineering
Massachusetts Institute of Technology
Cambridge, MA 02139

ABSTRACT

Experimental and theoretical studies on the turbulent combustion process have been done on a constant volume combustion bomb.

The flow into and out of the combustion bomb is computer controlled by specific valve opening and closing sequences. The nominal turbulent intensity in the bomb depends on the time delay after all valves are closed. Combustion experiments using a premixed propane-air mixture at equivalence ratios of 1.1, 1.0, and 0.95 have been performed in conjunction with spark delay times of 30 to 240 msec which correspond to a three fold variation in nominal turbulent intensity. The study focuses on the regime where the nominal initial turbulent intensity is about twice the laminar flame speed, which commonly arises in spark ignition engines. The behaviors of the mass burned fraction, front position, and turbulent burning speed, S_b are analyzed to extract general features of the underlying turbulent combustion process.

A time scaling parameter linearly dependent on the initial turbulent intensity, Z, scales both the mass fraction burned, and flame position data.

It is shown that if the burning speed, S_b, is a function of local properties, then the turbulent intensity ahead of the flame front is linearly proportional to the initial turbulent intensity. This greatly restricts the possible turbulence theories for the combustion process in internal combustion engines.

INTRODUCTION

The transient combustion process in an internal combustion engine can be classified into four stages according to the development of the combustion zone: (1) ignition; (2) flame development; (3) flame propagation; (4) flame termination. The third stage, flame propagation, is the focus of this paper.

It is widely recognized that turbulence in the combustion chamber has a profound influence on the flame propagation. In spite of much effort, a completely satisfactory model of the turbulent flame propagation has not been developed. The turbulent entrainment model proposed by Blizard and Keck (1) requires a relationship that connects the turbulent entrainment velocity u_e, the turbulent length scales, l_e, to engine geometry and operating conditions. However, results from experiments conducted by McCuiston et al (2) indicate that the assumptions of constant characteristic burn time τ and constant turbulent entrainment speed u_e are not correct. Tabaczynski et al (3) attempted to correct the theory by dividing the combustion process into a burning phase of a single eddy and a fully developed propagating combustion phase. This resulted in good agreement for burn durations.

Alternatively, Beretta, Rashidi, and Keck (4) developed a set of empirical equations for calculating the mass burning rates in SI engines. We use the same definition as (4) in the next section: the difference between u_b, the flame expansion speed, and the burning speed, S_b, is the unburned gas speed ahead of the flame front, U_g.

We will use the Rapid Distortion Theory (RDT) to calculate the turbulent intensity ahead of the flame front. The theory, developed by Prandtl (5) and Taylor (6), Batchelor and Proudman (7) and Townsend (8), is based on a local linearization, around a time or ensemble averaged flow. It is valid when the distortion of turbulence due to the changes in the mean flow is more rapid than the decay of turbulence due to the interactions between the eddies. In addition, the turbulent Reynolds number must be large ($Re \gg 1$), so that the viscous effects do not play a significant role.

The theory requires as inputs the strain rates of the deterministic mean motion and the initial state of turbulence. A feature of RDT is the linear relationship between the initial turbulent intensity and the turbulent fluctuations that arise later in the flow. For recent reviews of RDT with a discussion of its application to turbulence in compressible flows see Hunt (9) and Goldstein (10).

Wong and Hoult (11) reported a theoretical study (simulating the combustion process) of RDT. The theory assumes that the strain field is established by the expanding, time dependent, flame front. This motion is called the base flow (see Eq. (2)). The equations of motion are linearized about this base flow. In an engine, the theory predicts that the turbulent intensity ahead of the flame front is amplified rapidly by approximately a factor of two over its value before the start of combustion.

Ballal and Lefrebvre (12-18) conducted experiments in a constant pressure square duct. When $u' \approx 2S_l$ and $\eta \approx \delta_l$, where u' is the turbulent intensity, S_l is the laminar flame speed, η is the Kolmogoroff microscale, and δ_l is the flame

thickness, the turbulent flame is dominated by a turbulent diffusion process. When $u' > 2S_l$, $\eta << \delta_l$, the combustion zone is observed to be a thick matrix of burned gases interspersed with eddies of the unburned mixture. It is these two regimes which seem closest to the flame propagation which arises in IC engines, and in the present experiments.

Dyer (19) performed a series of experiments in a constant volume combustion bomb, where, in addition to the initial chemical and thermodynamic states of the mixture, the fluid motions at the time of ignition inside the bomb were measured, to provide data for validation of turbulent combustion models. However, the base flow is unknown in this experiment.

To test for the existence of the base flow, and for the predictions of RDT, a pancake-shaped combustion bomb with central spark plugs was constructed. Due to the geometry chosen, one can calculate the base flow from first principles. Bland (20) measured the steady flow field of the bomb while the valves are open. These measurements define the generation of turbulence by the intake process. Imoehl (21) used a moving hot wire to determine the decay of turbulence after the closing of inlet and exhaust valves. This defines the turbulent field at the start of combustion. Barraclough (22), and Nguyen (23) performed a series of combustion experiments using a premixed propane-air gas at equivalence ratios from 1.1 to 0.95. These define the scaling of the combustion process, our present topic.

Witze, Martin, and Borgnakke (24) measured the "mean" velocity and turbulent intensity ahead of the flame front of a single-cylinder spark ignition engine. Results indicate that there is no large turbulent amplification during the combustion (only a 30% increase). In addition, Lancaster's results (25) suggest that there is no amplification of turbulent intensity ahead of the flame front. For these reasons, we do not believe that the amount of amplification in RDT is correct.

In this paper, the RDT is extended by introducing modifications which take into account non-homogeneities in the initial turbulent state in the bomb (see the next section). The modifications do not lower the amplification by a factor of 3 to 10 required to be consistent with other experiments (24,25). In the same section, we also present calculations where the initial turbulence is passively convected by the base flow, with no amplification. The latter calculations are consistent with the results of Witze et al (24) and Lancaster (25). The bomb experiments (reported in the Experiment section) show that there is a universal scaling of pressure rise and of front position with initial turbulent intensity. Analysis of this result (in the Time Scaling Parameter section) show that the underlying turbulence theory must be linear if the turbulent burning velocity depends on local properties (a common assumption: see Refs. 1,2,3,4,11,25,26). This is the major result of this paper.

THEORETICAL CONSIDERATIONS

The calculations presented here are done for a constant volume right cylindrical combustion chamber with the spark plug located on the cylinder axis. Referring to Fig. 1, the following

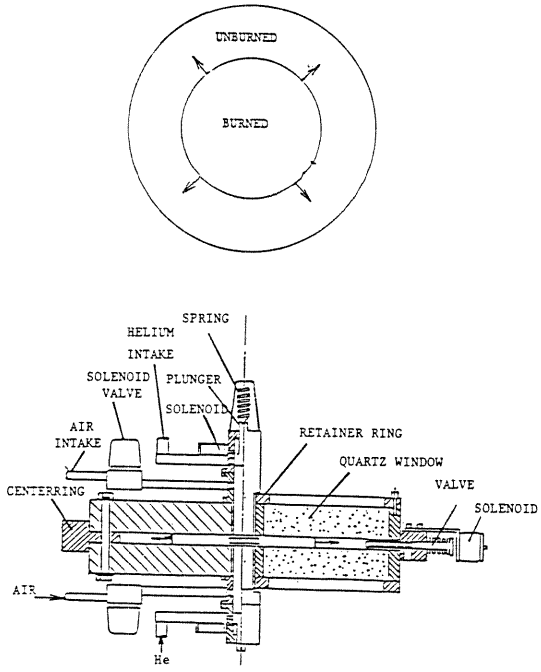

Fig. 1 Schematic of the flame propagation

assumptions are made to analyze the essential mechanics of the flow field as the combustion occurs:

(a) The flow is divided into two regions, an unburned gas region and a burned gas region, separated by a thin flame front occupying a negligible volume. The pressure is the same in both regions, and in each region, the temperature is uniform, as the gases are assumed to be completely mixed.

(b) The flame is a fully developed, therefore, the ignition delay is excluded. The flame front is cylindrical and concentric with the cylinder.

(c) The aspect ratio, h/D, where h is the height of the combustion bomb, D is the diameter, is small. The flow is treated as two-dimensional, axisymmetric, and purely radial flow. For the present experiment, h/D= 0.05.

(d) The unburned and burned gases obey the ideal gas law.

(e) The unburned gas is compressed isentropically by the expanding flame front.

(f) There is no heat loss to the environment. The uncertainty in equivalence ratio (about 10%) and the uncertainty in initial gas temperature (about 2%) preclude any accurate correlation of heat transfer in the present experiment (heat flux to the wall and temperature were not measured directly in the present experiment).

As the flame front propagates, the turbulent flow field ahead of the flame front is being compressed. The strain field is determined solely by the change in the unburned gas density and by the intial conditions. Using RDT (11,26), the properties of the turbulent flow field ahead of the flame front can be calculated from the strain field.

The local deterministic mean motion, U_r, or the fluid motion ahead of the flame front, is prescribed using (c), and the continuity equation. In cylindrical coordinates, the equation is written as follows:

$$\frac{1}{r}\frac{d}{dr}(rU_r) = -\frac{1}{\rho_u}\frac{d\rho_u}{dt} \qquad (1)$$

The solution of Eq. (1) subject to the boundary condition $U_r=0$ at the wall (r=R), assuming irrotational flow, is (26):

$$U_r = \frac{1}{2}\frac{1}{\rho_u}\frac{d\rho_u}{dt} R \left(\frac{R}{r} - \frac{r}{R}\right) \qquad (2)$$

The mass burned fraction is calculated using (a),(b),(d),(e),(f). The conservation of mass combined with the conservation of energy give the mass burned fraction (27):

$$x_b = \frac{P - P_0}{P_f - P_0} \qquad (3)$$

The burned gas radius, r_b, is determined by the conservation of mass in the bomb. This relationship is independent of the rate of burning. r_b is related to the density change and x_b as follows:

$$r_b = R \cdot \sqrt{\frac{\rho_u/\rho_0 - 1 + x_b}{\rho_u/\rho_0}} \qquad (4)$$

where R is the chamber radius. A complete derivation of Eq. (4) is given in Ref. 23.

The motion of the flame in a confined volume is complicated by the fact that the expansion of the burned gas compresses the unburned charge. Consequently, the thin boundary that separates the unburned gas and the flame front moves relative to the combustion chamber. The observed flame velocity (from Schlieren movie) is the sum of two velocities: the rate at which the flame moves into the unburned gas, called the burning velocity; and the rate at which the flame front is pushed forward by the expansion of the burned gas, called the base flow. In scalar form, the observed flame velocity is expressed as follows:

$$V_{obs} = S_b + U_r \qquad (5)$$

Solving for the burning speed, S_b,

$$S_b = V_{obs} - U_r \qquad (6)$$

where U_r is obtained from Eq. (2).

Another definition of the burning speed is given by Beretta, Rashidi, and Keck (4) as follows:

$$\frac{dm_b}{dt} = 2\pi h \rho_u r_b S_b = \frac{d(x_b \cdot m_0)}{dt} \qquad (7)$$

Using the conservation of mass, it can be shown that S_b has the form:

$$S_b = \frac{R \cdot \left(\frac{dx_b}{dt}\right)}{2\left(\frac{\rho_u}{\rho_0}\right)\left(\frac{r_b}{R}\right)} \qquad (8)$$

Equation (8) is equivalent to Eq. (6) using U_r (Eq. (2)). A complete proof is given in Ref. 23.

A useful form for S_b is (23):

$$S_b = \frac{dr_b}{dt} \cdot \frac{1+[(\rho_u/\rho_b - 1)\cdot x_b]}{\rho_u/\rho_b} \qquad (9)$$

Equation (9) is used by Beretta, Rashidi, and Keck (4). However, the common assumption of constant density ratio ρ_u/ρ_b is not correct. In our experiment the ratio varies from 5.5 to 3.2.

The Lagrangian path of a fluid particle is calculated by assuming that the particle moves with the base flow. The Euler-Lagrange equation of the particle can be written as:

$$\frac{dr(\underline{r}_0,t)}{dt} = U_r(\underline{r},t) \qquad (10)$$

or

$$\frac{dr}{dt} = \frac{1}{2}\frac{1}{\rho_u}\frac{d\rho_u}{dt} R \left(\frac{R}{r} - \frac{r}{R}\right) \qquad (11)$$

Integrating Eq. (11) yields

$$r(r,t\,|\,r_0,t_0) = \sqrt{\frac{\rho_0}{\rho_u} r_0^2 + R^2\left(1 - \frac{\rho_0}{\rho_u}\right)} \qquad (12)$$

Equation (12) is a statement of conservation of mass for the fluid in the control volume bounded by the cylinder wall and by the cylindrical surface of radius equal to that of the moving particle.

The Euler-Lagrange equation is used to determine a fluid particle's trajectory ahead of the flame front.

For a given burned gas radius, r_b, at a given time, t, during combustion, one can calculate the initial position of a fluid particle, r_0, which arrives at the flame front at time t. Equation (12) yields as follows:

$$r_0 = \sqrt{\frac{\rho_u}{\rho_0} r_b^2 - R^2\left(\frac{\rho_u}{\rho_0} - 1\right)} \qquad (13)$$

where r_b is given by Eq. (4).

The evolution of the fluctuating vorticity is governed by the interaction between the main turbulent motion and the base flow. For the present base flow according to RDT (11,26), the linearized vorticity transport equation can be expressed as follows:

$$\frac{D(\underline{\omega}'/\rho_u)}{Dt} = \left(\frac{\underline{\omega}'}{\rho_u} \cdot \nabla\right)\underline{U} \qquad (14)$$

The solution of Eq. (14) is written in the form:

$$\frac{\omega_i(\underline{x},t)}{\rho_u} = \frac{\omega_{0j}}{\rho_0}\gamma_{ij} \qquad (15)$$

where

$$\gamma_{ij} = \frac{\partial x_i}{\partial x_{0j}}(\underline{x}_0,t) \qquad (16)$$

is the distortion tensor. It is clear that given the Lagrangian description of a fluid particle, $\underline{x}_i(t)$ as a function of $\underline{x}_0$, t, and the initial state of turbulence, the vorticity can be determined at any later time.

In cylindrical coordinates, Eq. (16) is expressed as follows:

$$\gamma_{ij} = \begin{pmatrix} (r_0/r_b)\cdot(\rho_0/\rho_u) & 0 & 0 \\ 0 & r_b/r_0 & 0 \\ 0 & 0 & 1 \end{pmatrix} \qquad (17)$$

where r_0/r_b is given by Eq.(13) normalized by r_b.

Examining Eq. (17) indicates that the strain

field depends only on the density change and the ratio of the radial position (the independence theorem, Ref. 11).

Wong and Hoult (11) and Hoult and Wong (26) described how to calculate the velocity field which results from a given inital velocity, in the case where the turbulence is initially homogeneous and locally isotropic.

To apply this theory to the non-homogeneous case, we assume that the gradient in turbulent intensity is small ($h/D<<1$), so that we may consider the turbulence as locally homogeneous and isotropic. The radial variations in u' are assumed to be convected by the base flow and amplified as if the turbulence were homogeneous. The inviscid wall effects described by Wong (28) are ignored.

Figure 2 shows plots representing Eqs. (4) and (13). The solid lines represent the trajectories of fluid particles from three different initial locations for ϕ=0.95 and 1.1. Equation (13) can be explained pictorially as follows: at a given r_b, the initial location of a fluid particle can be determined by starting from the intersection point of its trajectory and the flame, r_b, and tracing the trajectory back to the beginning of the combustion (x_b=0), where $r=r_0$. This initial location, r_0/R_0, gives the initial non-dimensional location of the particle, and hence, the initial normalized turbulent intensity, as given by Eqs. (21) and (22).

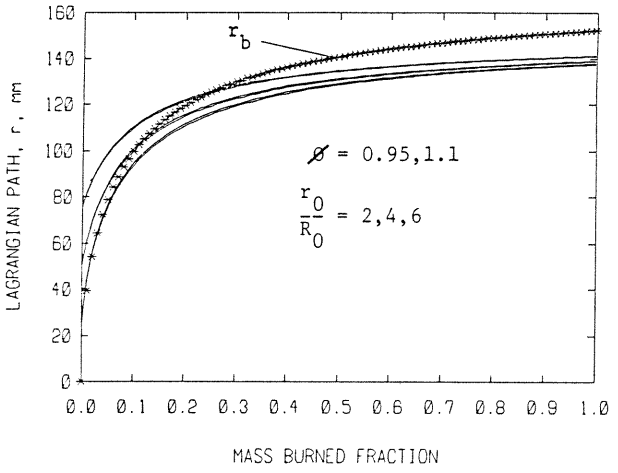

Fig. 2

The mass fraction burned is a function of spark delay and ignition delay times. Since the study only concerns with the propagating stage, the origin of the mass fraction burned versus time of each run is shifted to a new location on the time axis where it corresponds to the total decay time.

To non-dimensionalize the time axis, a scaling parameter called the shifted turbulent time, Z, is introduced and equal to:

$$Z = \frac{Tu'_0}{h} + \text{constant} \qquad (18)$$

where T represents the elapsed time (msec) from the new origin (T= t-total decay time), and h is the height of the combustion bomb and is the largest turbulent length scale in the experiment.

The total decay time will be defined in the next section. A small non-dimensional constant is required in order to collapse all the curves at Z= 0.60. The magnitude of the constant is of the order of the uncertainty in valve closing time.

Figures 3 and 4 show the radial (rr) and theta ($\theta\theta$) components of the distortion tensor obtained from Eq. (17) as functions of Z. These components and the value of initial turbulent intensity are

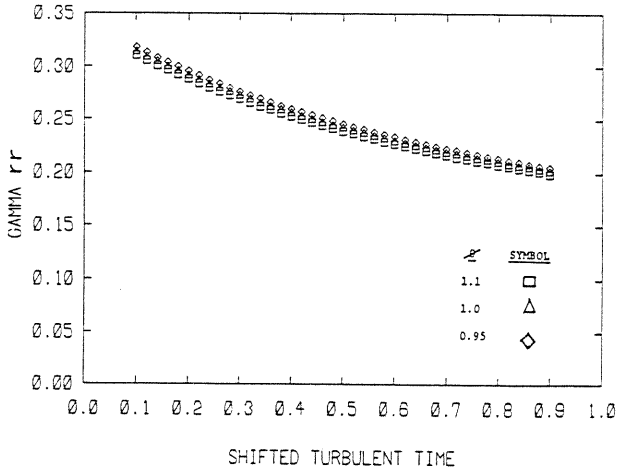

Fig. 3

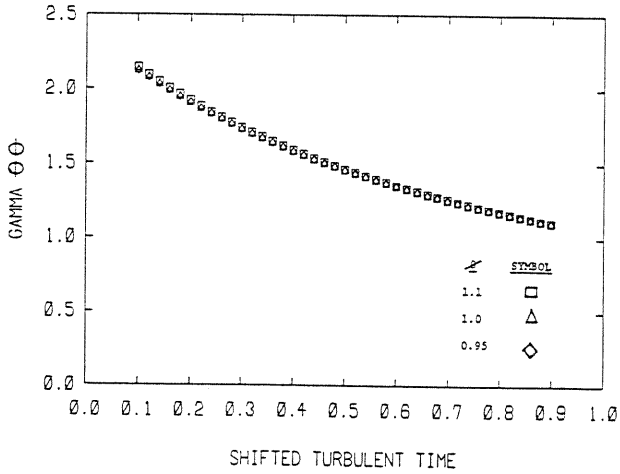

Fig. 4

used in RDT to calculate the turbulent intensity at the flame front. The process of convection of the initial turbulent intensity by the base flow and amplification according to RDT may be mathematically stated as:

$$u' = u'_0 \cdot A'_{RDT} \cdot \sqrt{F[(r_b, t\ r_0, t_0)/R_0]} \qquad (19)$$

Here, A'_{RDT} denotes the amplification of the nominal initial value of turbulent intensity, as calculated from an analytical expression (11,26) for the homogeneous case. Figure 5 shows u'/u'_0, where u'_0 is defined in Eq. (23), as function of Z for three equivalence ratios. The amplification, the ratio u'/u'_0, rises slowly and levels off from Z of 0.45 to 0.55, then decreases, reflecting the

initial gradient in turbulent intensity, $F(r/R_0)$ (Eq. (22)).

The turbulent intensity at the flame front can also be calculated from the convection of the base flow alone. The pure convection calculation is presented as a limiting case, to contrast with the prediction from RDT. The turbulent intensity, in this case, is expressed as follows:

$$u' = u'_0 \cdot \sqrt{F[(r_b, t\ \ r_0, t_0)/R_0]} \qquad (20)$$

In order to compare with Eq. (19), Eq. (20) is normalized with u'_0 and is plotted against Z for three equivalence ratios in Fig. 6. The turbulent intensity is lowered by a factor of three and the curves are almost identical.

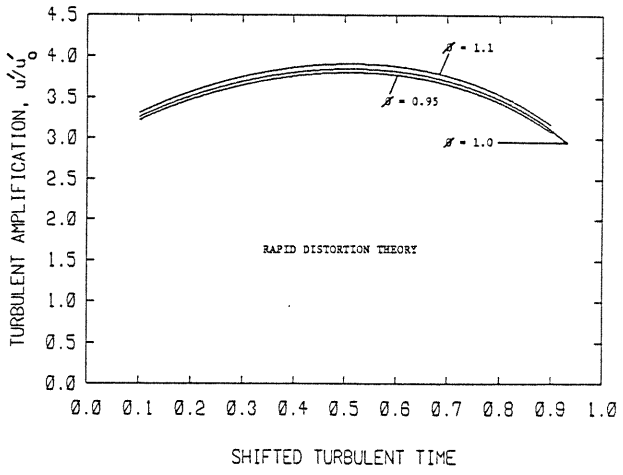

Fig. 5

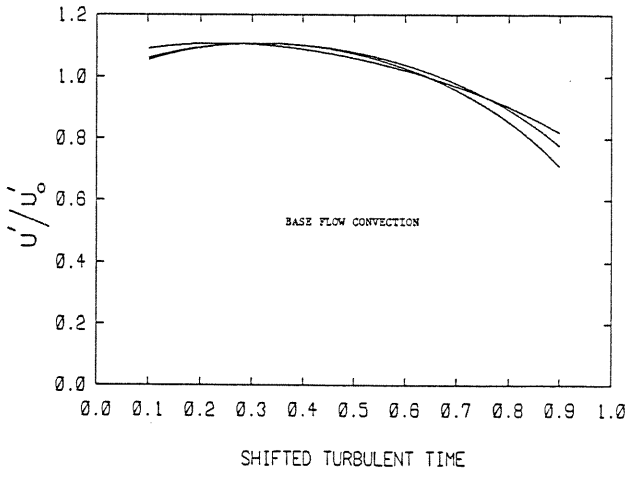

Fig. 6

Figure 7 shows a flow chart of calculating the turbulent intensity from any turbulence theory. The program requires as input the initial value of turbulent intensity. The program is then initialized at the start of the combustion process (x_b=t=0). Following the initial conditions are the thermodynamic calculations, in which the density ratio of the unburned gas is determined. Using this density ratio, the burned gas radius is calculated. The "x_b Lagrange" calculations determine the initial location of a fluid particle and the corresponding value of $F(r/R_0)$ as described by Eq. (22). Calculations are performed to find the evolution of turbulence from RDT (Eq. (19)) or from base flow convection (Eq. (20)). The burn time is calculated next by using a burn law. Burn laws are thoroughly reviewed by Andrews et al (29). Once the burn time is known, the trajectory of the fluid particle is determined from the Lagrangian time calculations. An incremental value of mass burned fraction is added and the entire loop starts over again until the completion of the combustion process.

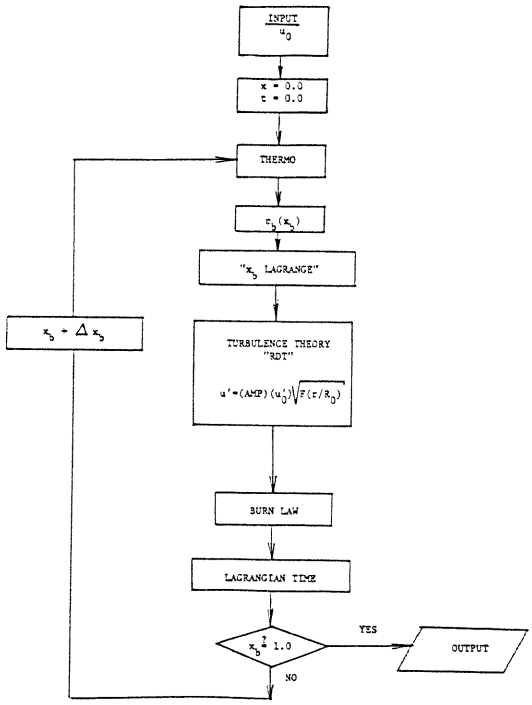

Fig. 7

EXPERIMENT

Combustion Chamber

The combustion bomb is a right circular cylinder with aspect ratio (height/diameter) of 0.05. The bomb consists of two identical flat circular stainless steel plates bolted together to form the top and bottom of the cylindrical chamber. The height of the bomb is 15.875 mm and the diameter is 304.8 mm. Two quartz windows, located on the top and bottom plates, provides optical access to the chamber. Top and side views of the bomb are shown in Figs. 8 and 1, respectively. A hot wire access port is located 6° offset from one of the exhaust valves. A similar port is located 180° from the first port. In addition, a hot wire access in the axial direction is provided through four ports in one of the windows.

Centrally mounted on the top and bottom plates are the intake valves as shown in Fig. 1. The inlet valves are equipped with four optical interrupters to determine the valve closing times.

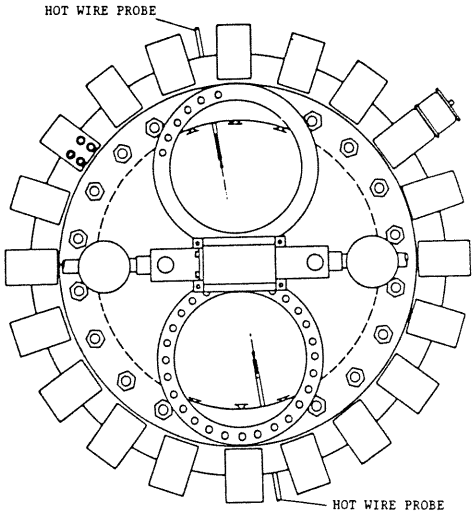

Fig. 8 Top view of the combustion bomb

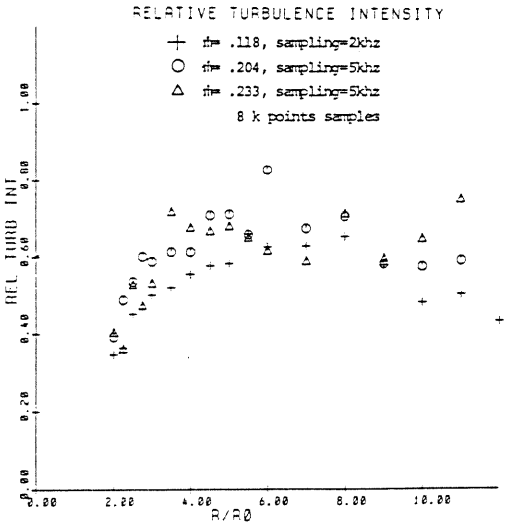

Fig. 9

Five volt pulses generated from these interrupters are recorded on a oscilloscope and the closing times are then determined. The mean closing times of the top inlet valve is 12 msec and of the bottom inlet valve is 14 msec. The standard deviations of both valves are 3.2 msec.

Twenty equally spaced automotive-type poppet valves are located 18° apart on the perimeter of the bomb. Each valve is assembled to a fast response-time solenoid. A mean closing time of all the valves is about 40 msec, and the standard deviation is 1.0 msec. The lift of each valve is set separately for equal mass flow rate with equal pressure drop.

Generation of Turbulence by the Intake Process

The flow field in the combustion bomb while the valves are open, steady state conditions, has been studied (20). The standard corrections (30-32) were made for the high turbulent intensity level found in the bomb. To stabilize the flow, flow straighteners are suspended from the center of the bomb by pins. These pins are staggered 60° out of phase to minimize the effects of wake in the flow field (Fig. 1).

The relative turbulent intensities for three mass flow rates are shown in Fig. 9. The radial position is normalized by the inlet throat radius. The normalized intensities rise sharply and then level off at roughly 0.5.

Turbulent Decay Rate

The decay in turbulent energy is determined by closing the valves after establishing the intake flow, and measuring the decaying random velocity field with the moving hot wire (21). The moving hot wire is calibrated with the probe velocity. Mean turbulent intensities are calculated from ensemble averages of data from 15 sets of 100 runs at 14 different traverse delay times. In each run, the mass flow rate is 0.09 kg/sec. The normalized turbulent intensity fits a power law of the form:

$$\left(\frac{u'}{U_0}\right)^2 = 0.007 \cdot F(r/R_0) \cdot \left(\frac{tU_0}{R}\right)^{-1.13} \qquad (21)$$

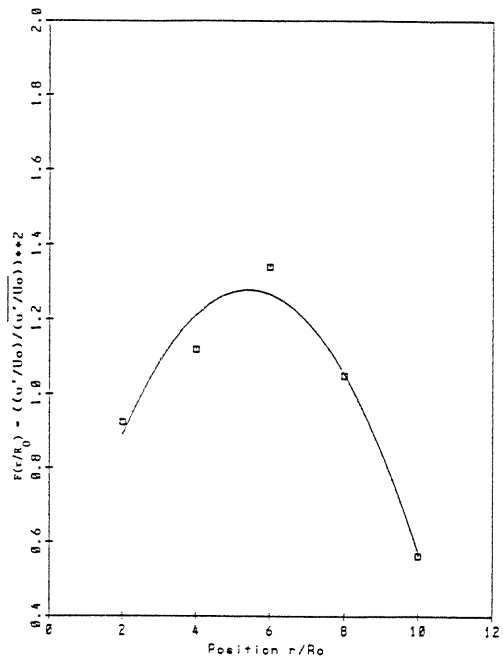

Fig. 10 Radial dependence of turbulent energy with second order fit

where $F(r/R_0)$ is the radial dependence of the turbulent energy, U_0 is the throat velocity, R_0 is the throat radius, and R is the bomb radius.

Figure 10 shows $F(r/R_0)$ as a function of the normalized radial time. Also, $F(r/R_0)$ is given a second order fit of the form:

$$F\left(\frac{r}{R_0}\right) = 0.41 + 0.29\left(\frac{r}{R_0}\right) - 2.56\times10^{-2}\left(\frac{r}{R_0}\right)^2 \qquad (22)$$

Pressure and Mass Fraction Burned

A series of combustion experiments using a premixed propane-air gas at equivalence ratios of 1.1 to 0.95 were performed (22,23).

To study the effect of turbulence on

combustion, the spark delay time is varied, thus varying the initial turbulent intensity seen by the combustion process, as described by Eqs. (21) and (22). The spark delay time is the elapsed time in msec from valve closing to when a spark signal is generated. The total decay time is the sum of the spark delay time and the time it takes the pressure in the bomb to rise 30% above the initial pressure. This time is substituted into t in Eq. (23) to calculate the nominal initial turbulent intensity, where $F(r/R_0) = 1.0$. The nominal initial turbulent intensity, which is used as a scaling velocity, is from Eq. (21):

$$u'_0 = [0.007 \cdot U_0^2 \cdot (\frac{tU_0}{R})^{-1.13}]^{1/2} \qquad (23)$$

Table 1 lists the experimental conditions for each run.

Table 1 Experimental conditions

Run	ϕ	Spark Delay(msec)	u'_0(m/sec)
1	1.1	30	1.10
2	1.1	60	0.77
3	1.0	30	1.06
4	1.0	60	0.75
5	1.0	120	0.52
6	0.95	30	0.90
7	0.95	60	0.66
8	0.95	120	0.46

Flame Position and Flame Thickness

Each frame of the flame front from Schlieren movie is projected upward on a flat and transparent table by a 45° flat mirror located below the table. On the image, three azimuthal lines, 12° apart, are drawn with the middle line coincides the center line of the bomb. The flame leading and trailing density gradients are measured and converted to the laboratory coordinates.

The flame radius is the average of the leading and trailing density gradients . In runs 6, 7, and 8, the trailing density gradients could not be determined, as a result, the leading density gradients are represented as the flame radii.

TIME SCALING PARAMETER

A plot of mass fraction burned versus Z is shown in Fig. 11. Also, a solid line is added to the plot to represent the universal fit of all data points. The formula of the fit is given in Ref. 23.

Examination of Fig. 11 indicates that from Z of 0.1 to 0.9, the curves are virtually identical. Although they are some deviations beyond 0.9, they do not appear to be systematic. It is concluded that x_b is scaled with Z.

A plot for flame position versus Z, using the same constant as before, are shown in Fig. 12. Similar to Fig. 11, a solid line is included in each plot to represent the universal fit of all data points. The formula of the fit is given in Ref. 23.

The front position is not as well defined as the pressure, because the front thickness is quite variable, being about 0.8h. In Fig. 12, the data scales with Z, for Z from 0.1 to 0.9 as in Fig. 11. For small Z, the front positions in run 5 do not follow the scaling--this corresponds to frames

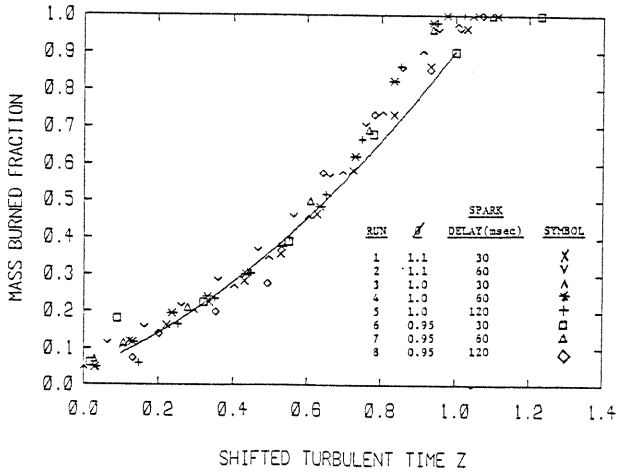

Fig. 11

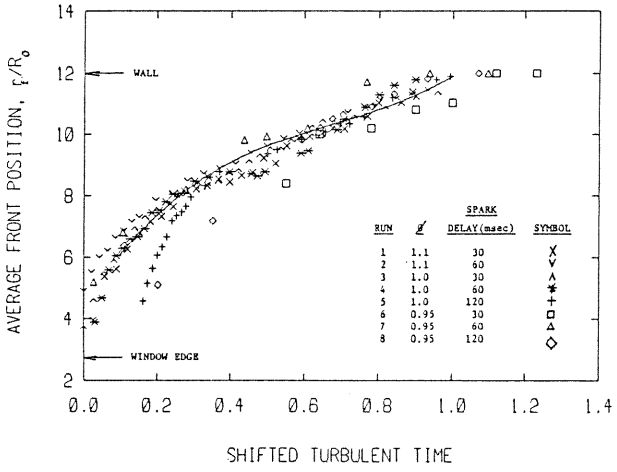

Fig. 12

A and B of Fig. 13. Runs 6, 7, and 8 lack trailing density gradient data--if a thickness estimate were included in the leading density gradient data then these data are indistinguishable from the other runs. Within the accuracy of the data, both pressure and flame position scale with Z. The constant in the definition of Z (see Eq. (18)) is the same for pressure as it is for the front position, in each run.

Table 2 lists the ratio of the initial turbulent intensity to the initial laminar flame speed of each run. The laminar flame speed is obtained from Metghalchi and Keck (33).

Table 2 Values of u'_0/S_{l_0}

Run	ϕ	S_{l_0} (m/sec)	u'_0/S_{l_0}
1	1.1	0.39	2.82
2	1.1	0.39	1.97
3	1.0	0.38	2.78
4	1.0	0.38	1.97
5	1.0	0.38	1.35
6	0.95	0.37	2.43
7	0.95	0.37	1.77
8	0.95	0.37	1.25

The initial turbulent intensities are approximately twice the initial laminar flame speeds, thus, it indicates that the combustion occurs in the region called transition region discussed in the Introduction.

Examining Fig. 13 demonstrates the behavior of the flame front. Figure 13 is a series of still pictures made from the Schlieren movie and corresponds to run 3. The flame front is thick and its surface is irregular at early stage of its propagation (frame A). This is in a region where the two flame fronts, arising from the two spark plugs, meet as they travel through the flow straighteners (Fig. 1). A short distance downstream of the flow straighteners the front becomes thin and the flame surface is very smooth as seen in frame B. Then, the flame front progressively thickens and wrinkles as shown in the remaining frames. For similar ratios of u'_0/S_{l0}, Ballal and Lefrebvre (12-18) report that the burning process is controlled by two mechanisms: (i) the flame front is wrinkled by eddies that are larger than the flame thickness; (ii) small pockets of unburned gas are entrained within the reaction zone.

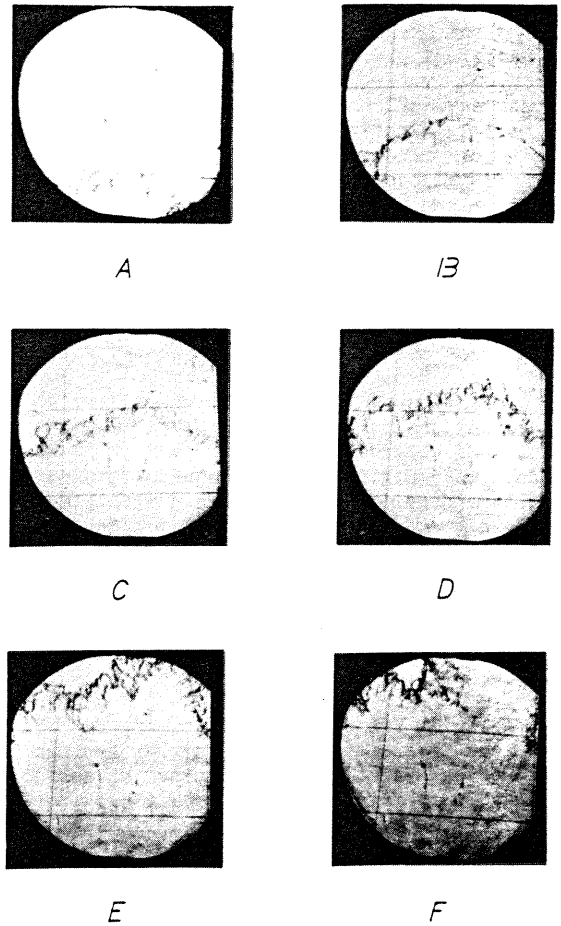

Fig. 13 Schlieren photographs of 30 msec spark delay combustion, ϕ = 1.0

A plot of r_b, burned gas radius, versus r_f, observed flame radius, is shown in Fig. 14. The burned gas radius is essentially the same as the flame radius. Hence, the two-zone thermodynamics model represents this experiment with adequate accuracy. A corollary is that the values of V_{obs} (see Eq. (5)) obtained by using either r_b or r_f are equivalent.

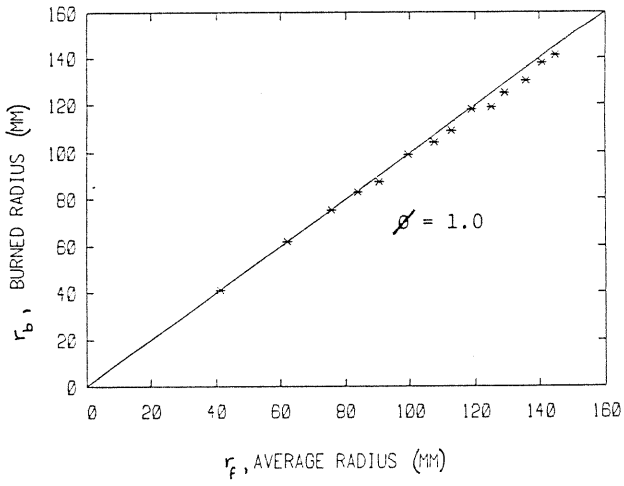

Fig. 14

A plot of S_b normalized by u'_0 versus Z for three equivalence ratios is shown in Fig. 15. Equation (8) is used and note that S_b varies linearly with u'_0.

Equation (5) is solved for the base flow,

$$U_r = V_{obs} - S_b \qquad (24)$$

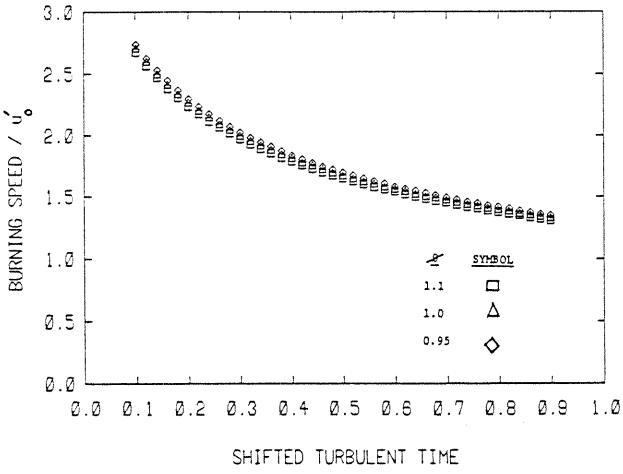

Fig. 15

Figure 16 shows the base flow as a function of Z obtained from Eq. (24). The solid line is obtained by using dr_b/dZ, and the circled line is obtained by using dr_f/dZ. In both cases the universal fit of mass fraction burned is used to calculate S_b.

The base flow at the flame front agrees with the simple one-dimensional theory, and the two-zone thermodynamics model.

An examination of the flow chart (Fig. 7) shows that the only way that the Z scaling can

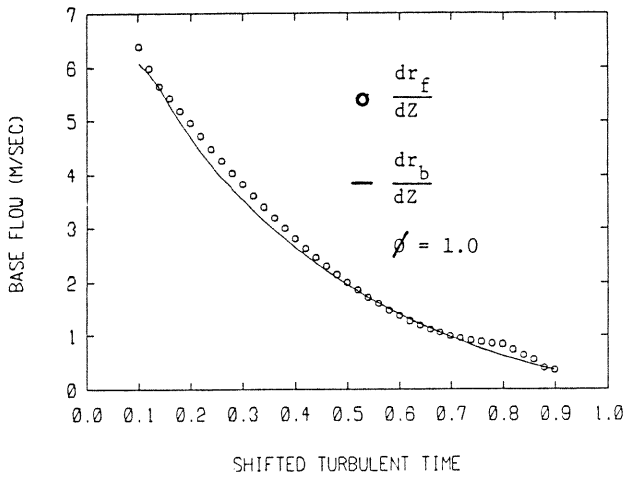

Fig. 16

arise is if S_b is linearly dependent on u'_0. If it is assumed that S_b depends on local properties, i.e., that the combustion process is unaffected by motions more than a clearance height, h, away from the front, then the turbulent intensity at the flame front must depend linearly on u'_0. This in turn implies that a turbulence theory, whatever its form, must have a similar linear property.

Examining Fig. 15 along with Fig. 4 suggests that the burning speed may be a function of the distortion tensor in the θ-direction. We believe that the decrease in value of $Y_{\theta\theta}$ causes the flame front to form "little fingers" and to open up these fingers at later stage of flame propagation (Fig. 13). A plausible turbulent burning law might be:

$$Sb \sim A \cdot u' \cdot Y_{\theta\theta} \qquad (25)$$

where A is a constant.

Figure 17 shows a comparison of S_b calculated from Eq. (25) and from the experimental data. Using RDT, the values of the curve with A=0.39 are within 30% of the experimental values. Using base flow convection, the values of the curve with A=1.21 show similar agreement.

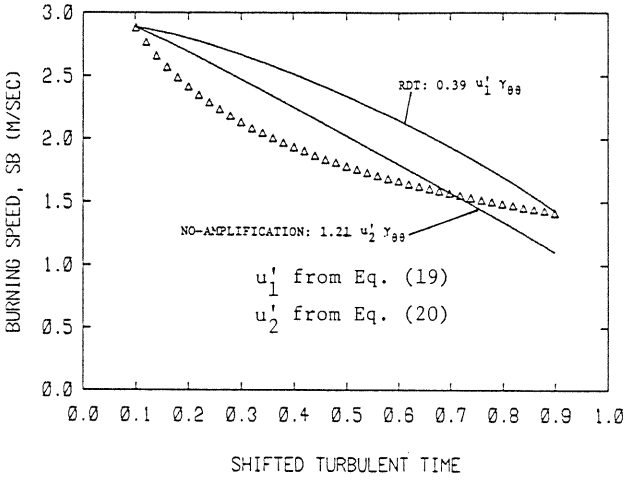

Fig. 17 A comparison between theory and experiment

CONCLUSIONS

The following conclusions are drawn from the study:

1. Two definitions of the burning speed, S_b, which are given by the vector analysis of the observed flame motion and by thermodynamics, are equivalent.
2. $r_b \approx r_f$, therefore, the two-zone thermodynamic model is valid, within the accuracy of the experiment.
3. The observed base flow agrees well with the predicted baseflow.

A linear time scaling with the initial turbulent intensity is obtained because:

4. The mass burned fraction, x_b, is scaled with Z.
5. The average flame radius, r_f, is scaled with Z.

The Z scaling requires that any turbulence theory to have the following characteristic:

$$S_b \propto u'_0 \qquad (26)$$

Furthermore, if S_b is a function of local properties, then the following statement can be made:

$$u' \text{ at flame front} \propto u'_0 \qquad (27)$$

Equation (27) implies that the turbulent theory describing the flow ahead of the flame front must yield a turbulent intensity which is linearly dependent on the initial turbulent intensity in the combustion bomb. This fundamental conclusion is the main contribution of this paper.

Townsend (8) showed that a linear eddy viscosity dampens the strained turbulence behind a grid in a wind tunnel with a contraction while preserving the shape of the eddy. Perhaps a similar correction is required for the RDT applied to closed volume combustion. Such a correction would preserve the linear scaling which seems to be required while dealing with the effects of rapid distortion.

ACKNOWLEDGEMENT

This work is supported by the Department of Energy's Lean Engine Efficiency Program under contract number DE-AC04-81AL16310.

REFERENCES

1. Blizard, N. C., and Keck, J. C., "Experimental and Theoretical Investigation of Turbulent Burning Model for Internal Combustion Engines," SAE Trans. Vol. 83, Paper No. 740191, pp. 846-864, 1974.
2. McCuiston, F. D., Lavoie, G. A., and Kauffman, C. W., "Validation of a Turbulent Flame Propagation Model for a Spark Ignition Engine," SAE Trans. Vol. 86, Paper No. 770045, pp. 200-223, 1977.
3. Tabaczynski, R. J., Ferguson, C. R., and Radhakrishnan, K., "A Turbulent Entrainment Model for Spark-Ignition Engine Combustion," SAE Trans. Vol. 86, Paper No. 770647, pp. 2414-2433, 1977.
4. Beretta, G. P., Rashidi, M., and Keck, J. C., "Turbulent Flame Propagation and Combustion in Spark Ignition Engines," Combustion and Flame 52, pp. 217-245, 1983.

5. Prandtl, L., "Attaining a Steady Air Stream in Wind Tunnels," NACA TM 726, 1933.
6. Taylor, G. I., "Turbulence in a Contracting Stream," Zeit. F. Angew. Math. U. Mech. 15, p.91, 1935.
7. Batchelor, G. K., and Proudman, I., "The Effect of Rapid Distortion of a Fluid in Turbulent Motion," Quart. Journ. Mech. and Applied Math., Vol. VII, Part 1, pp. 83-103, 1954.
8. Townsend, A. A., The Structure of Turbulent Shear Flow, Cambridge University Press, Cambridge, Second Edition, pp. 80-88, 1976.
9. Hunt, J. C. R., "A Review of the Theory of Rapidly Distorted Turbulent Flows and Its Applications," paper presented at the XIII Biennial Fluid Dynamics Symposium. Advanced Problems and Methods in Fluid Mechanics, Poland, September 1977.
10. Goldstein, M. E., "Unsteady Vortical and Entropic Distortions of Potential Flows Round Arbitrary Obstacles," J. Fluid Mech., Vol. 89, Part 3, pp. 433-468, 1978.
11. Wong, V. W., and Hoult, D. P., "Rapid Distortion Theory Applied to Turbulence Combustion," SAE Trans. Vol. 88, Paper No. 790357, pp. 1243-1262, 1979.
12. Ballal, D. R., and Lefrebvre, A. H., "Turbulence effects on Enclose Flames," Acta Astronautica, Vol. 1, pp. 471-483, Pergamon Press, 1974.
13. Ballal, D. R., and Lefrebvre, A. H., "The Structure and Propagation of Turbulent Flames," Proc. R. Soc. Lond. A 344, pp. 217-234, 1975.
14. Ballal, D. R., "An Experimental Study of Flame Turbulence," Acta Astronautica, Vol. 5, pp. 1095-1112, Pergamon Press, 1978.
15. Ballal, D. R., "The Structure of a Premixed Turbulent Flame," Proc. R. Soc. Lond. A 367, pp. 353-380, 1979.
16. Ballal, D. R., "The Influence of Laminar Burning Velocity on the Structure and Propagation of Turbulent Flames," Proc. R. Soc. Lond. A 367, pp. 485-502, 1979.
17. Ballal, D. R., "Further Development of the Three-Region Model of a Premixed Turbulent Flame--I. Turbulent Diffusion Dominated Region 2," Proc. R. Soc. Lond. A 368, pp. 267-282, 1979.
18. Ballal, D. R., "Further Development of the Three-Regiion Model of a Premixed Turbulent Flame--II. Instability Dominated Region 1," Proc. R. Soc. Lond. A 368, pp. 283-293, 1979.
19. Dyer, T. M., "Characterization of One-and-two-Dimensional Homogeneous Combustion Phenomena in a Constant Volume Bomb," SAE Trans. Vol. 88, Paper No. 790353, pp. 1196-1216, 1979.
20. Bland, C. C., "Flow Characterization of a Turbulent Combustion Bomb," M.S. Thesis, Dept. of Mech. Engrg., M.I.T., 1981.
21. Imoehl, W. J., "A Study of Turbulence Decay in A Turbulent Combustion Bomb," M.S. Thesis, Dept. of Mech. Engrg., M.I.T., 1982.
22. Barraclough, S., "A Comparison Between a Propane-Air Combustion Front and a Helium-Air Simulated Combustion Front," M.S. Thesis, Dept. of Mech. Engrg., M.I.T., 1983.
23. Nguyen, V. H., "A Turbulent Burning Law Derived from Combustion Bomb Experiments," M.S. Thesis, Dept. of Mech. Engrg., M.I.T. 1985.
24. Witze, P. O., Martin, J. K., and Borgnakke, C., "Conditionally-Sampled Velocity and Turbulence Measurements in a Spark Ignition Engine," Combustion Sci. Tech., Vol. 36, pp. 301-307, 1984.
25. Lancaster, D. R., "Effects of Engine Variables on Turbulence in a Spark Ignition Engine," SAE Trans. Vol. 85, Paper No. 760159, pp. 671-688, 1976.
26. Hoult, D. P., and Wong, V. W., "The Generation of Turbulence in An Internal-Combustion Engine," Modeling in Reciprocating Engines, (Mattavi, J. N. and Amann, C. A. eds.) Plenum Press, New York, pp. 131-160, 1980.
27. Taylor, C. F., The Internal Combustion Engine in Theory and Practice, M.I.T. Press, Vol. 2, p. 13, 1980.
28. Wong, V. W., "Distortion of Turbulence in a Reciprocating Engine Cylinder," Ph.D. Thesis, Dept. of Mech. Engrg., M.I.T., 1979.
29. Andrews, G. E., Bradley, D., and Lwakabamba, S. B., "Turbulence and Turbulent Flame Propagation--A critical Appraisal," Combustion and Flame 24, pp. 285-304, 1975.
30. Acrivlellis, M., and Felsch, K. O., "New Method of Determining the Flow Field with Low and High Turbulent Intensity," presented at the Joint/ASME/CSME App. Mech., Fluids Eng., Bioeng. Conf., Niagara Falls, NY, June 18-20, 1979, Publ. by ASME, pp. 169-177, 1979.
31. Durst, F., and Rodi, W., "Evaluation of the Wire Signals in Highly Turbulent Flows," Fluid Dynamic Measurements in the Industrial and Medical Environments Proc., Disa Conf., NY, Humanities Press, 1972, held at University of Leicester, England, April 12-14, p. 343, 1972.
32. Champagne, F. H., and Sleicher, L. A., "Turbulence Measurements with Inclined Hot Wires," J. Fluid Mech., Vol. 28, Part 2, pp. 177-182, 1967.
33. Metghalchi, M., and Keck, J. C., "Laminar Burning Velocity of Propane-Air Mixtures at High Temperature and Pressure," Combustion and Flame 39, pp. 143-154, 1980.